On welding defect detection and causalities between welding signals

Abdallah Amine Melakhsou, Mireille Batton-Hubert

On welding defect detection and causalities between welding signals

Abdallah Amine Melakhsou[1] Mireille Batton-Hubert[2]

Abstract—In the manufacturing of hot water tanks, welding quality evaluation and fault detection is a critical operation that is still frequently conducted visually or with the help of none destructive tests, which can generate a high consumption of time and resources. To overcome this problem, many methods have been proposed for defect detection based on the classification of the welding signals. However, most of the proposed methods do not consider the problems of defect localization and the generalization from small sample size. Moreover, studies on the interactions between welding signals seem to be absent in the literature despite its importance in the formulation of the defect detection problem. In this paper, we aim to address these gaps by presenting a study on the causalities between welding signals in the circular welding of hot water tanks. Based on the findings from the causality study, we propose a method that detects and localize welding defect with high accuracy and handles the problem of small sample size. Furthermore, we present a study on the defects root cause and show the possibility of early defect prediction.

Keywords: Welding defect detection; Signal decomposition; Causality.

I. INTRODUCTION

Welding fault detection and quality evaluation are still often performed visually or using nondestructive examination. Industries for which welding is a main task, namely hot water tanks industry, are in need for less expensive and less time-consuming strategies to conduct these missions. Using welding signals, many works have been carried out for welding fault detection employing signal processing and machine learning techniques. Huang [1] proposed a Support Vector Machine (SVM) model based on the multi-scale entropy of the current and voltage signals that detects three types of defects. Arabaci & Laving [2] carried out a study to categorize welding defects from raw current signals using principal component analysis. Pernambuco [3] used Artificial Neural Network for the classification of sound signals to detect the absence of shielding gas. After decomposing current signals into intrinsic mode functions (IMFs) by the empirical mode decomposition method, Huang [4] suggested an SVM model based on features selected from some IMFs to detect porosity under pulsed TIG.

Despite the significant number of works carried out on the subject, there are still some gaps such as the problem of defect localization, the generalization from small training

This work was supported by elm.leblanc. France

sample and the study of defects root cause from the signals. Moreover, we notice from the literature that most of the proposed methods for welding defect detection are based on the classification of some statistical features extracted from the signals, which may not lead to a sufficient accuracy especially that the characteristics of the signals can change over time. A more robust strategy for defect detection is then needed. Zhang [5] stated that welding process has a high complexity of randomness and interference. We believe that a robust strategy for defect detection must address this randomness and the interactions between the welding parameters during the welding operation in order to achieve high accuracy detection.

Relation between welding parameters and weld quality in the offline mode is a subject that is widely studied in the literature for the purpose of optimizing some quality criterion. Experiment design methods and meta-models like Taguchi and Kriging were used in a considerable number of works in order to correlate welding parameters (voltage, current, wire feed speed, welding speed,...) with the geometry of the weld [6][7] and the work-piece distortion [8][9] resulting from the welding operation. However, to the best of our knowledge, no work has been done to study interactions between parameters during the welding cycle despite its importance for gaining better understanding of the welding dynamics and the information contained in the signals in order to have a better formulation of the problem of welding defect detection. This can be achieved using methods of causality analysis on the welding signals.

Causality between time series has been and still an active research subject. The first causality concept was formalized by Granger in 1968. The concept states that there is causality between two time series if the knowledge of both their past reduces the prediction error of one of them. Since then, many causality measures have been proposed from different science fields such as Information Theory and Chaos Theory. Among the information theory causality measures, Transfer Entropy (TE) introduced by Schreiber [10] has gained a lot of interest and has been used in multiple disciplines such as physiological signals analysis for emotion recognition [11] and brain disorders recognition [12]. In engineering, TE was used successfully for fault root cause diagnosis [13][14] and early fault detection in rotating machinery [15].

[1] Abdallah Amine Melakhsou is a PhD student at the Faculty of Mathematical and Industrial Engineering, Ecole´ des Mines de Saint-Etienne,´ 158 Cours Fauriel, 42023 Saint-Etienne.´ France. amine.melakhsou@emse.fr

[2] Mireille Batton-Hubert is a Professor at Mines Saint-Etienne, Univ Clermont Auvergne, CNRS, UMR 6158 LIMOS, Institut Henri Fayol, F - 42023 Saint-Etienne France batton@emse.fr

In the present paper, we aim to fill the discussed gaps in the literature which are :

- The fact that most of the proposed methods for defect detection are based on features extraction from the signals, which may not provide a good discrimination, namely because of the feature selection problem and the one known as curse of dimensionality,
- The absence of welding defect detection methods able to generalize from small training sample,
- The fact that most of the proposed methods do not address the problem of defect localization,
- The absence of the study on the interactions between welding parameters during the welding cycle,
- The absence of the study on defects root cause from the signals as most of the studies were conducted on deliberately made defects.

We attempt to fill these gaps by studying the interactions between welding electrical signals obtained from the circular welding of hot water tanks, which we carry out using concepts of causality and signal decomposition. Based on the findings of causalities, we then derive an interpretable method for welding defect detection and localization based on the classification of the probability density function of one of the IMFs of the voltage signal. We show that our methodology outperforms previous ones and that it can handle the problem of small sample size. Moreover, we present a study on the defects root cause based on the signals and confirm the possibility of early defect prediction.

The remainder of the paper is organized as follows. In section 2 we describe the theoretical framework of the methods we use for causality and signal decomposition. In section 3 we present the circular welding process of hot water tanks. We present the results of causality, derive the defect detection, the defect localization method and present a study on defects root cause in section 4. Finally, we give a conclusion and discuss future works.

II. METHODS

A. Transfer Entropy

Transfer Entropy (TE) is a non-parametric causality measure from the information theory field that was proposed by Schreiber [10]. It detects linear and non-linear causalities between time series. For the calculation of TE, the time series are considered stationary Markov processes. The TE from a time series Y to X (the amount of information transferred from Y to X) is given by:

$$TE_{Y->X} = \sum p(X_{n+1}, X_n^k, X_n^l) log \frac{p(X_{n+1}|X_n^k, Y_n^l)}{p(X_{n+1}|X_n^k)} \quad (1)$$

where:

- X_n, Y_n are the processes X and Y at time n
- k,l are the order of the Markov processes X and Y respectively. Chosen to be 1 in our work.

If Y does not cause X, the conditional probability $p(X_{n+1}|X_n^k, Y_n^l)$ is equal to $p(X_{n+1}|X_n^k)$, the TE is then null, which indicates no information flow from Y to X. It was shown by Marsbinski & Kantz [16] that the estimate of TE given in (1) can be biased due to small sample effects. A solution that they proposed is called Effective Transfer Entropy (ETE) which is given in (2):

$$ETE_{Y->X} = TE_{Y->X} - TE_{shuffled} \quad (2) \quad Y \dashrightarrow X$$

where $TE_{Y \xrightarrow{shuffled} X}$ is the TE with the shuffled time series (random drawings from the time series). This approach is a block bootstrap that can be used to evaluate the statistical significance of the information flow. We use 100 shuffles in our study. To estimate TE and ETE, several approaches can be used to estimate the probability distributions. We use in our study the histogram method.The optimal number of the histogram binsi estimated by:

$$bins = \sqrt{\frac{N}{5}} \quad (3)$$

where N is the length of the time series. This estimate simulates the method proposed by Cellucci et al. [17] for adaptive binning. We utilize the package *RTransferEntropy* [18] that implements estimation of TE and ETE based on the histogram method.

B. Variational mode decomposition

Variational mode decomposition (VMD) is a novel adaptive signal decomposition method developed by Dragomiretskiy & Zosso [19]. VMD decomposes a signal $f(t)$ into k quasi-orthogonal sub-signals $u_k(t)$ called Intrinsic Mode Functions (IMFs). Unlike other adaptive decomposition methods like Empirical Mode Decomposition, VMD has a theoretical formulation and the obtained modes are bandlimited. VMD is given as a constrained variational problem that minimizes the modes' spectral bandwidths using the H^1 Gaussian smoothness, given by:

$$\min_{u_k(t),\omega_k} \sum_k \left\| \partial t(\delta(t) + \frac{j}{\pi t}) * u_k(t) e^{-i\omega_k t}) \right\|_2^2$$
$$s.t \sum_k u_k = f \tag{4}$$

where :

- $\delta(t)$ is the Dirac distribution
- $u_k(t)$ is the k^{th} IMF
- ∂ denotes the partial derivative
- $(\delta(t)+\frac{j}{\pi t})*u_k(t))$ is the Hilbert transform of the mode $u_k(t)$
- ω_k is the center frequency of the mode $u_k(t)$
- f is the signal to be decomposed

The problem is addressed using quadratic penalty and Lagrangian multiplier. The Augmented Lagrangian is given by:

$$\begin{aligned} L(u_k, \omega_k, \lambda) =& \alpha \sum \left\| \partial t(\delta(t) + \frac{j}{\pi t}) * u(t)_k \exp^{-i\omega_k t} \right\|_2^2 \\ &+ \left\| f(t) - \sum_k u_k \right\|_2^2 \\ &+ \langle \lambda(t), f(t) - \sum_k u_k \rangle \end{aligned} \tag{5}$$

where α is a penalty term used to control the spectral bandwidths of the modes and λ is the Lagrangian multiplier used to emphasizes the signal reconstruction constraint.

The problem is then solved using alternate direction method of multipliers (ADMM). The mode u_k is estimated in the frequency domain by:

$$\hat{u}_k(\omega) = \frac{\hat{f}(\omega) - \sum_{i \neq k} \hat{u}_i(\omega) + \hat{\lambda}(\omega)/2}{1 + 2\alpha(\omega - \omega_k)^2} \tag{6}$$

where

- $\hat{u_k}(\omega)$ is the Fourrier transform of the k^{th} mode
- $\hat{f}(\omega)$ is the Fourrier transform of the signal to be decomposed
- $\hat{\lambda}(\omega)$ is the Lagrangian multiplier which is equivalent to Wiener filter. The center of gravity ω_k of the spectrum of k^{th} mode is obtained by:

$$\omega_k = \frac{\int_0^\infty \omega |u_k(\omega)|^2 d\omega}{\int_0^\infty |u_k(\omega)|^2 d\omega} \tag{7}$$

the Lagrangian multiplier $\hat{\lambda}(\omega)$ is updated in the iterative algorithm following the formula:

$$\hat{\lambda}(\omega)^{n+1} \leftarrow \hat{\lambda}(\omega)^n + \tau(\hat{f}(\omega) - \sum_{i=k} \hat{u_i}(\omega)) \tag{8}$$

where n is the number of iterations and τ a parameter that controls the signal reconstruction. Further information and discussions on the method can be found in [19].

In the next section, we describe the circular welding of hot water tanks for which the study is carried out.

III. DESCRIPTION OF THE CIRCULAR WELDING PROCESS IN THE MANUFACTURING OF HOT WATER TANKS

A hot water tank undergoes several welding processes. We study in this paper the circular welding that assembles the cylinder and the two caps simultaneously as shown in Fig. 1. This is performed by a semi-automatic machine employing Tungsten Inert Gas (TIG) welding. When the welding cycle starts, an electrical arc that produces the heat for the fusion is ignited between the electrode and the work-piece. A servomotor is used to guide the wire into the welding pool. A shielding

gas composed of Argon and Nitrogen is used to protect the weld pool from oxidation. The current can be pulsed or constant depending on the type of the water tank.

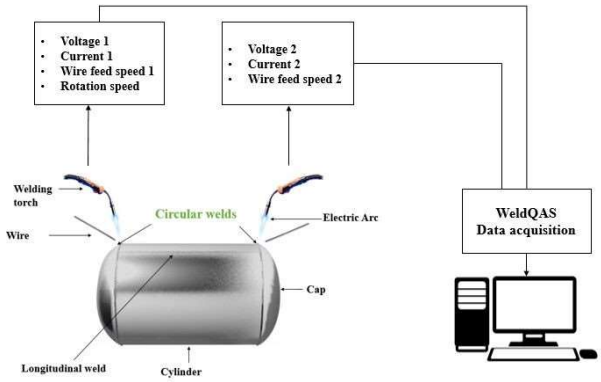

Fig. 1. Illustration of the circular welding system.

During the cycle, the torches are immovable while the hot water tank automatically rotates.

We consider in the study two different hot water tanks made respectively of austenitic stainless steel and Duplex stainless steel. Information on welding parameters for both products are summarized in Table I.

TABLE I

INFORMATION ON WELDING PARAMETERS

	Current type	Current (A)	Voltage (v)	Wire speed (m/min)
Austenitic	Pulsed at f=7Hz	190	10.5	8
Duplex	Constant	180	10	8.5

In addition to the signal of the tank's rotation speed, signals of voltage, current and wire speed are acquired for the two circular welding using WeldQAS data acquisition device with a sampling rate of 25Hz. All the signals used in this work were recorded from welding tanks destined to the final customers. We do not carry out experiments since we are interested in capturing the real behaviour of the system.

IV. RESULTS

A. Causalities between welding signals

TE is applicable only for stationary time series. However, welding signals may be non-stationary. To overcome this limitation, differencing or de-trending non-stationary signals are often used to make them stationary [21]. We propose to use VMD to decompose the signals and remove the trends whenever the signal is non-stationary. This can be achieved by choosing the center frequency ω_1 of the first mode to be at 0 Hz so that it perfectly captures the trend.

We begin by investigating causality between voltage and wire speed signal in the case of welding austenitic hot water tanks. The current signal being constant will not be considered. Fig. 2 (a) shows the voltage and Fig. 2 (d) the wire speed signal. To verify the non-stationarity of the voltage signal we apply the Augmented Dickey Fuller (ADF) test to test stationarity against the null hypothesis that the time series has a unit root which implies the non-stationary. We obtain a p-value of 0.5354, which indicates that the time series is non-stationary. We then apply VMD with k=5, α=500 and τ=2 to force the signal reconstruction. The first mode is shown in Fig. 2 (b). The voltage signal without the trend mode shown in Fig. 2 (c) will be used for the causality detection. The wire speed signal in Fig. 2 (d) is stationary, the application of the ADF test gives a p-value of 0.01. Therefore, we do not remove the trend.

Table II shows the results of the application of Transfer Entropy for these signals. We obtain an ETE of 0 for voltage→−wire speed and a value of 0.0149 with a p-value of 0.01 in the opposite direction. These results indicate that in this case, the wire speed causes changes in the voltage signal but not vice-versa. This shows the interference of the

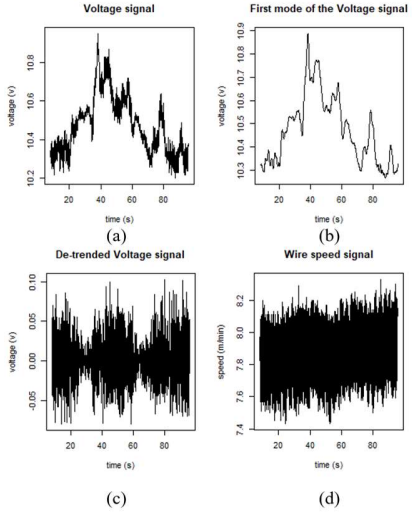

Fig. 2. (a) Voltage signal. (b) First mode of the voltage signal. (c) voltage signal without the first mode. (d) Wire speed signal.

wire in the electric arc, whose dynamics are explained by the voltage signal.

Let us now study signals in the case of defective welding with burn-through. Fig. 3 (a) shows a voltage signal where a defect occurs at the 26^th second characterized by the peaks. Its trend component is shown in Fig. 3 (b). The signal without the trend is shown in Fig. 3 (c) and the corresponding wire speed signal in Fig. 3 (d). We notice that the wire speed signal exhibits also an abnormal behavior at the same time as the defect occurrence. An interesting question to ask is if this anomaly in the wire signal caused the defect. ETE values in Table III indicate that the voltage signal causes the wire speed signal, the $ETE_{Voltage \rightarrow Wire}$ is non null and a p-value slightly above 5%. We understand from this result that the burn-through appears first in the voltage signal then propagates to the signal of the wire speed since the voltage signal causes the wire speed signal. The causality in the opposite direction is non significant.

Following the same methodology, we study causalities between signals obtained from welding a Duplex hot water tank. Both circular welds were defective. For this instance we include the current signal as the welding was carried out using pulsed current. We also acquired signal of the welding speed that will be included in the causality study.

Fig. 4. shows the voltage, current and wire speed signals obtained for each of the two circular welds. The welding speed signal in Fig. 5 is common for the two sides as both welds are performed simultaneously.

TABLE II

RESULTS OF TRANSFER ENTROPY

Direction	TE	ETE	P value
$Wire \rightarrow Voltage$	0.9221	0.0149	0.0100
$Voltage \rightarrow Wire$	0.7924	0.0000	0.1167

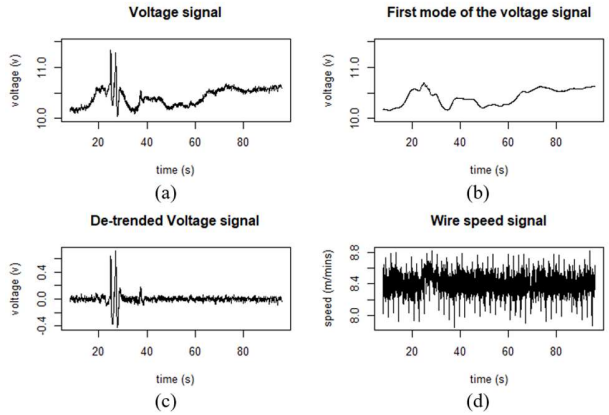

Fig. 3. (a) Voltage signal of defective weld. (b) First mode of the voltage signal. (c) voltage signal without the first mode. (d) Wire speed signal.

TABLE III

RESULTS OF TRANSFER ENTROPY ESTIMATED FOR THE DEFECTIVE WELD SIGNALS

Direction	TE	ETE	P value
$Wire \rightarrow Voltage$	0.0831	0.0000	0.3300
$Voltage \rightarrow Wire$	0.2562	0.0013	0.0767

TE results for these signals are given in Fig. 6 in a diagram form. For the signals of the right side weld, the interference of the current pulse frequency in the voltage signal is detected. This interference is well known to welding experts and scholars. Moreover, TE detects that voltage causes welding speed.

In addition to these two causalities, TE detects that the voltage causes the current signal for the left weld, which is an unexpected causality. After decomposing the left current signal using VMD, we noticed that the trend shows an anomaly (Fig. 7) at the same time as the defect appearance in the voltage signal, which explains the detected causality.

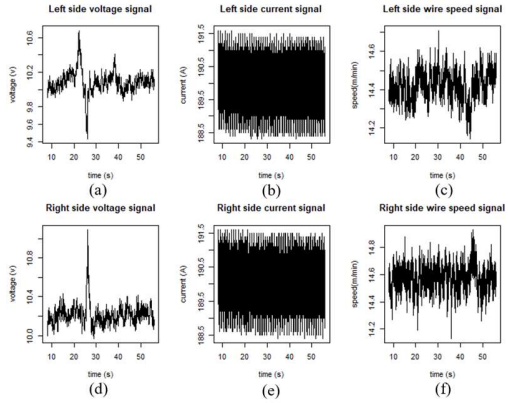

Fig. 4. (a) Left voltage signal. (b) Left current signal. (c) Left wire speed signal. (d) Right voltage signal.(e) Right current signal. (c) Right wire speed signal.

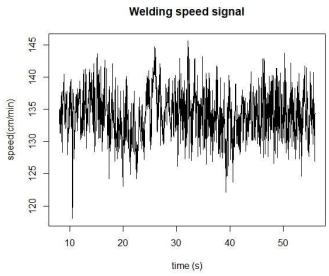

Fig. 5. Welding speed signal acquired during the welding of a Duplex hot water tank

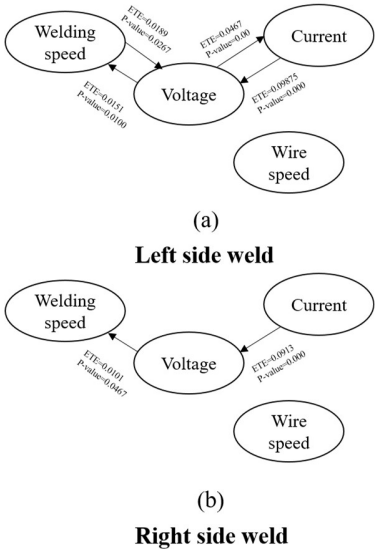

Fig. 6. ETE results given in a causality diagram.

This confirms again that the burn-through appears first in the voltage signal and that it is transmitted this time to the current signal.

TE shows also that in the left side weld, the rotation speed signal causes the voltage signal. This result has an explanation, in fact it is the left side of the machine that is motorized and drives the rotation of the hot water tank. We learn from this causality that the vibrations resulting from the rotation of the tank are transmitted to the electric arc.

Using VMD, we find that the trends of the left voltage signal and the rotation speed signal are negatively correlated (Fig. 8) with a correlation coefficient of -0.7059. This explains the causality voltage→ speed, which might indicate that the rotation speed is influenced by the amount of heat produced by the electric arc as it acts as a negative force for the rotation.

The application of the TE allowed us to gain a better knowledge of the signals of the circular welding of hot water tanks. From the above study we conclude that:

- When a burn-through occurs, it appears firstly in the voltage signal and can propagate to the other signals.
- When welding with pulsed current, the pulse oscilla-

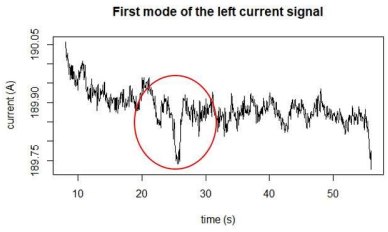

Fig. 7. Trend of the left current signal.

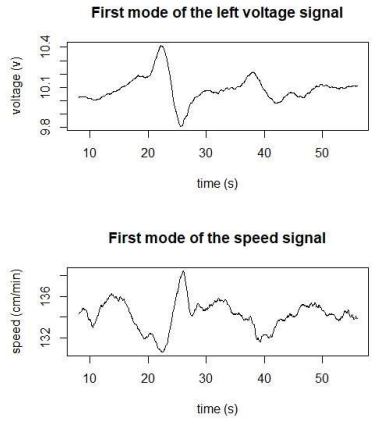

Fig. 8. Trends of the left voltage and speed signals

tions are present in the voltage signal.

- When welding with constant current, the voltage signal contains the oscillations of the wire feed speed.
- The vibrations generated by the tank rotation are transmitted to the voltage of the motorized side.
- The left voltage signal is negatively correlated to the signal of rotation speed.

These conclusions will allow us in the next section to define a method for welding defect detection and localization.

B. Welding defect detection

We saw from the previous section that the burn-through defect appears first in the voltage signal and is characterized by the peaks, which can be transmitted afterwards to the other signals. We propose in this paper to detect the defects from the voltage signals as they are more visible in them. We also concluded that the voltage signal contains oscillations originated from the wire, the current pulse and from the rotation of the tank.

We notice that we do not need all the components of the signal to detect the peaks. The trend component is irrelevant in this specific task. Other modes contain interference of the wire speed and the welding speed vibrations, in addition to the pulse oscillations when welding with the pulsed current as seen in the previous section. In order to obtain an accurate defect detection, discarding the uninteresting modes is an important step. We make use of the VMD method to extract only the mode we are interested in. In the frequency domain reflection, the peaks indicating the defect are rare events in the signal, they are then contained in a low frequency mode. The trend of the signal is in the first mode if we set its center gravity at 0Hz, the second mode contains then the rare events.

Fig. 9 shows two voltage signals of defective (Fig. 9 (a)) and good (Fig. 9 (b)) welds together with their respective second modes obtained by VMD (with the same parameters used in the previous section). We notice that this mode contains indeed the sudden peaks in the defective weld signal (Fig. 9 (c)) . For the good weld signal, the second mode (Fig. 9 (d)) is approximately a flat signal, which indicates that there were no defects.

A tool that can accurately capture the presence of peaks in a signal is the probability density function (PDF). This strategy was proposed in [20]. Fig. 10 shows the two probability functions estimated from the second mode of each of the studied signals. We notice that for the good weld, the PDF has Leptokurtic form indicating that all the values are within the mean. For the the defective weld, we remark that there are values that are so far from the mean. This confirms the presence of the sudden peaks in the mode. Thus the occurrence of a defect. Automatic PDF classification can be achieved employing curves classifier. In this paper, we use the functional non-parametric kernel classifier developed by Ferraty & Vieu [22]. The classifier is based on Bayes theorem. It estimates the posterior probability of the membership of a functional observation to the predefined classes. The posterior probability of an incoming instance is estimated as the odds ratio using the distances between the incoming instance and the training curves. A kernel is used to smooth the distances, We use in our model the Gaussian kernel since it provides the best accuracy. The curve is afterwards assigned to the class for which the posterior probability is the highest.

If we divide the defective mode into multiple segments using a sliding window and estimate the PDF for each of them, we can detect the ones that contain the sudden

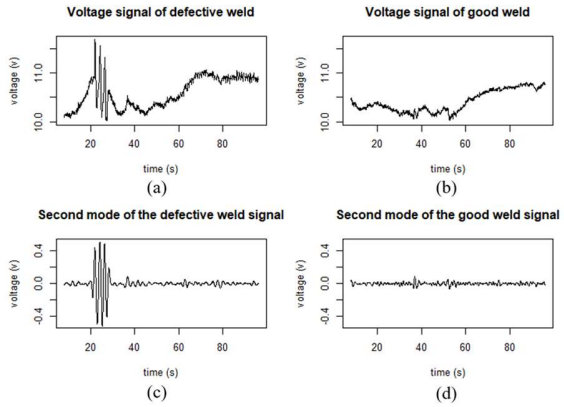

Fig. 9. (a) Voltage signal of a defective weld. (b) Voltage signal of a good weld. (c) Second mode the defective signal. (d) Second mode of the good weld signal.

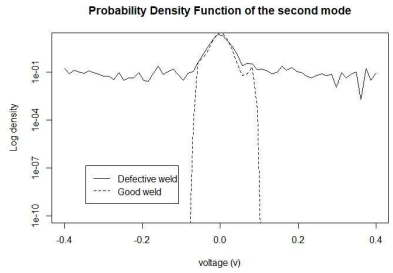

Fig. 10. Probability Density Functions of the two modes

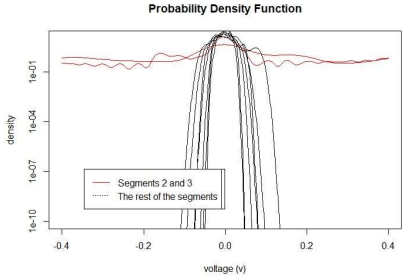

Fig. 11. Probability Density Functions of the mode's segments

peaks. Thus, achieving defect localization. The segments that contain the defect can be seen as smaller drawings from the PDF of the defective weld mode. The PDFs estimated from these segments will then resemble the one obtained for the defective weld mode.

Fig. 11 shows the PDFs estimated from segments consisting of 8 seconds of the defective mode shown in Fig. 9 (c). We can straightforwardly identify that the second and the third segments hold the defect signature.

Based on theses analysis, we define the methodology for defect detection and localization in Fig. 12. The voltage signal is firstly decomposed using VMD then the PDF of the second mode is estimated. This latter is classified as either belonging to defect-free weld or weld with burn-though. If it belongs to the defective class, the corresponding second mode is segmented and the PDF of each segment is classified using the same classifier. We use the same classifier since we concluded that PDFs of a defective weld signal and the ones estimated from segments containing the defect are very similar.

To create the model, we use 400 voltage signals, which is equivalent to 200 welding cycles of austenitic hot water tanks. Half of them correspond to nonconforming welds. To train the model, we use 70% of the signals with equitable partitioning of the two categories. For a comparative study, we use one of most used method in the literature, namely in a recent work by Moinuddin [23], which consists of classifying the signals based on a feature vector extracted from the raw signals and the

use of the SVM classifier. We choose a feature vector composed of the mean, standard deviation, energy and entropy of the raw voltage signals.

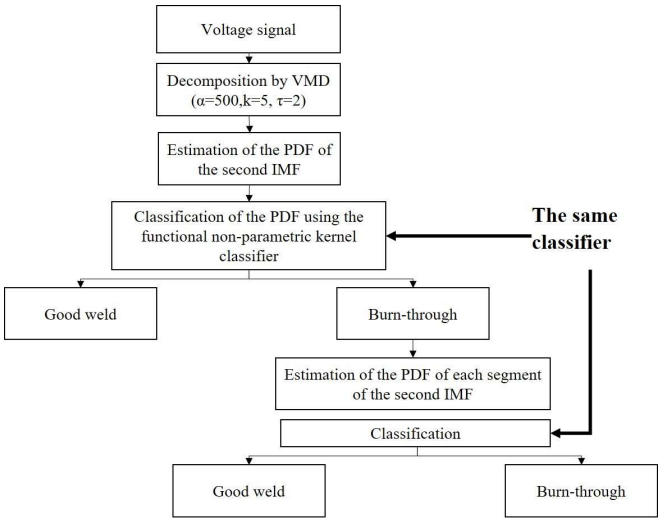

Fig. 12. The proposed methodology for welding defect detection and localization.

TABLE IV

ACCURACY OF THE PROPOSED MODEL

	Training		Test	
	Good	Defective	Good	Defective
Good	138	2	58	2
Defective	3	137	0	60
Accuracy	98.21%		8.3%	

TABLE V

ACCURACY OF THE SVM MODEL

	Training		Test	
	Good	Defective	Good	Defective
Good	123	51	52	24
Defective	17	89	8	36
Accuracy	75.71%		73.33%	

validation of our methodology and the one based on the feature extraction and SVM. We obtain a validation accuracy of 98.3% using the presented methodology, which outperforms the second strategy that fails to properly discriminate the signals and has 73.33% accuracy.

Collecting and labeling welding signals can be a timeconsuming and a tedious step. The presented methodology can handle the problem of small sample size thanks to the good discrimination between the two categories. To show that, consider training both our model and the SVM model and using only 5% of the data-set, which corresponds to 20 signals (10 defective welds, 10 good welds). Tables VI and VII show the results of our model and the SVM model for this partitioning. Only 10 signals out of 380 are misclassified using our model in the validation while the SVM model misclassifies 114 signals. This confirms the ability of our strategy to generalize from a small training sample.

Tables IV and V show the accuracy for the training and the

TABLE VI

ACCURACY OF THE PROPOSED MODEL TRAINED ON A SMALL SAMPLE

	Training		Test	
	Good	Defective	Good	Defective
Good	10	0	185	5
Defective	0	10	5	185
Accuracy	100%		97.36%	

	Training		Test	
	Good	Defective	Good	Defective
Good	9	3	184	108
Defective	1	7	6	82
Accuracy	80%		70%	

TABLE VII

ACCURACY OF THE SVM MODEL TRAINED ON A SMALL SAMPLE

In addition to the accurate classification achieved, the proposed methodology offers a highly dimensions reduction. The PDFs used for the classification consist of only 64 points while the original signals have a length of 2200 points. This leads to fast defect detection and localization, which meets the requirements of online monitoring.

C. Study of the defects root cause based on the signals

Using the presented methodology, we localized the burnthrough in 150 voltage signals. We are interested now in what happens in the signals before the defect occurrence because this can lead us to the defect root-cause. Using VMD, we obtained the trends of the signals at the defect localization. One can ask what is the common characteristic that these signal segments share? This can be answered using the method of time series shape extraction proposed by Paparrizos & Gravano [24]. This method finds a time series, which summarizes a time series set by maximizing the sum of a shape similarity measure based on cross-correlation (also proposed by the authors), which handles the distortions in shift and amplitude. Fig. 13 shows the extracted shape from the trends of the signals at the defect localization. We notice that a gradual increase before the defect appearance summarizes the set. Since the voltage signal is correlated to the arc length, the extracted shape shows that the arc lengthens before the defect occurs. This happens when there is a gap between the cap and the cylinder as shown in Fig.
14.

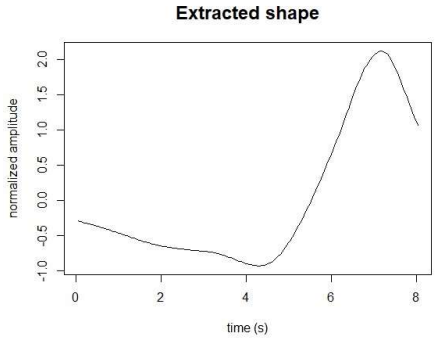

Fig. 13. The extracted shape from the signals of defective welds.

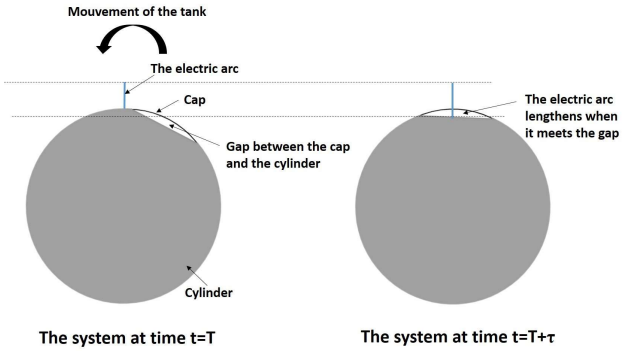

Fig. 14. Illustration of the misalignment between the cap and the cylinder.

The gap between the cap and the cylinder can be caused by bending imperfections or by the distortion that the cylinder could exhibit after the longitudinal welding. These geometrical imperfections must be addressed in order to reduce the burn-through in the circular welding.

We notice that the extracted shape does not only give us information on the defects root-cause, it also shows that it is possible to predict the defect by the early recognition of the gradual increase in the voltage signal. This is a major subject that we will study in future works.

V. CONCLUSIONS

In this paper, we studied the interactions between welding signals in the case of the circular welding of hot water tanks. Based on the conclusions of the causality study, we proposed a method capable of detecting and localizing burnthough with high accuracy. We showed that our methodology outperforms previous ones and that it can handle the problem of small sample size. Moreover, we presented a study on defects root cause based on the signals and showed the possibility of early prediction of welding defect. In future works, detecting other types of welding defects will be studied along with the detection of defects under other welding processes. Moreover, the results obtained from this study will be exploited for the subject of early welding defect prediction.

ACKNOWLEDGMENT

Authors would like to thank elm.leblanc France for the funding of this study and for the other resources they made available.

REFERENCES

[1] Huang, Y., Yang, D., Wang, K., Wang, L., & Zhou, Q. (2020). Stability analysis of GMAW based on multi-scale entropy and genetic optimized support vector machine. Measurement, 151, 107282.

[2] Arabaci, H., & Laving, S. Weld Defect Categorization from Welding Current using Principle Component Analysis.

[3] Pernambuco, B. S. G., Steffens, C. R., Pereira, J. R., Werhli, A. V., Azzolin, R. Z., & Estrada, E. D. S. D. (2019, October). Online Sound Based Arc-Welding Defect Detection Using Artificial Neural Networks. In 2019 Latin American Robotics Symposium (LARS), 2019 Brazilian Symposium on Robotics (SBR) and 2019 Workshop on Robotics in Education (WRE) (pp. 263-268). IEEE.

[4] Huang, Y., Wu, D., Zhang, Z., Chen, H., & Chen, S. (2017). EMDbased pulsed TIG welding process porosity defect detection and defect diagnosis using GA-SVM. Journal of Materials Processing Technology, 239, 92-102.

[5] Zhang, Z., Yang, Z., Ren, W., & Wen, G. (2019). Random forestbased real-time defect detection of Al alloy in robotic arc welding using optical spectrum. Journal of Manufacturing Processes, 42, 5159.

[6] Lim, N. K. (2014). Optimization of TIG weld geometry using a Kriging surrogate model and Latin Hypercube sampling for data generation. California State University, Long Beach.

[7] Yang, Y., Cao, L., Wang, C., Zhou, Q., & Jiang, P. (2018). Multiobjective process parameters optimization of hot-wire laser welding using ensemble of metamodels and NSGA-II. Robotics and ComputerIntegrated Manufacturing, 53, 141-152.

[8] Qing, W. A. N. G., Zhao, L. I. U., Pinghua, H. U. A. N. G., & Ping, Z. H. U. (2019). Distortion Prediction and Geometry Compensation Method for Laser Welding-Induced Distortion of Body-in-White. Journal of Shanghai Jiaotong University, 53(1), 62.

[9] Ansaripour, N., Heidari, A., & Eftekhari, S. A. (2020). Multi-objective optimization of residual stresses and distortion in submerged arc welding process using Genetic Algorithm and Harmony Search. Proceedings of the Institution of Mechanical Engineers, Part C: Journal of Mechanical Engineering Science, 234(4), 862-871.

[10] Schreiber, T. (2000). Measuring information transfer. Physical review letters, 85(2), 461.

[11] Gao, Y., Wang, X., Potter, T., Zhang, J., & Zhang, Y. (2020). Singletrial EEG emotion recognition using Granger Causality/Transfer Entropy analysis. Journal of Neuroscience Methods, 346, 108904.

[12] Dejman, A., Khadem, A., & Khorrami, A. (2017, May). Exploring the disorders of brain effective connectivity network in ASD: a case study using EEG, transfer entropy, and graph theory. In 2017 Iranian Conference on Electrical Engineering (ICEE) (pp. 8-13). IEEE.

[13] Ma, L., Dong, J., & Peng, K. (2018). Root cause diagnosis of qualityrelated faults in industrial multimode processes using robust Gaussian mixture model and transfer entropy. Neurocomputing, 285, 60-73.

[14] Jiao, J., Zhen, W., Zhu, W., & Wang, G. (2020). Quality-related Root Cause Diagnosis Based on Orthogonal Kernel Principal Component Regression and Transfer Entropy. IEEE Transactions on Industrial Informatics.

[15] Wu, Z., Zhang, Q., Wang, L., Cheng, L., & Zhou, J. (2018). Early fault detection method for rotating machinery based on harmonic-assisted multivariate empirical mode decomposition and transfer entropy. Entropy, 20(11), 873.

[16] Marschinski, R., & Kantz, H. (2002). Analysing the information flow between financial time series. The European Physical Journal BCondensed Matter and Complex Systems, 30(2), 275-281.

[17] Cellucci, C. J., Albano, A. M., & Rapp, P. E. (2005). Statistical validation of mutual information calculations: Comparison of alternative numerical algorithms. Physical Review E, 71(6), 066208.

[18] Behrendt, S., Dimpfl, T., Peter, F. J., & Zimmermann, D. J. (2019). RTransferEntropy—Quantifying information flow between different time series using effective transfer entropy. SoftwareX, 10, 100265

[19] Dragomiretskiy, K.,& Zosso, D. (2013). Variational mode decomposition. IEEE transactions on signal processing, 62(3), 531-544.

[20] Melakhsou, A.A., & Batton-Hubert, M. (2021). Welding monitoring and defect detection using probability density distribution and functional nonparametric kernel classifier. *Submitted for publication.*

[21] Bossomaier, T., Barnett, L., & Harre, M. (2013). Information and´ phase transitions in socio-economic systems. Complex Adaptive Systems Modeling, 1(1), 1-25.

[22] Ferraty, F., & Vieu, P. (2003). Curves discrimination: a nonparametric functional approach. Computational Statistics & Data Analysis, 44(12), 161-173.

[23] Moinuddin, S. Q., Hameed, S. S., Dewangan, A. K., Kumar, K. R., & Kumari, A. S. (2021). A study on weld defects classification in gas metal arc welding process using machine learning techniques. Materials Today: Proceedings, 43, 623-628.

[24] Paparrizos, J., & Gravano, L. (2015, May). k-shape: Efficient and accurate clustering of time series. In Proceedings of the 2015 ACM SIGMOD International Conference on Management of Data (pp. 18551870).